Composite Truss Bridge Decks

João Pedro Ribeiro Braz *

Instituto Superior Técnico, TULisbon, Portugal

Abstract

An experimental investigation was carried out in the aim to understand the behavior of a bridge deck consisting of a three-dimensional steel truss made composite with a concrete slab. This investigation consisted in constructing a test specimen and loading it to collapse by means of a static load control test.

A moment curvature analysis was performed in order to predict the ultimate capacity of the system. A relative good precision was achieved for the ultimate flexural capacity of the negative moment zones, as for the global vertical displacements. However, the structural system didn't maintain both strength and ductility up to the end of the test, due to local failure modes verified in several critical zones.

The results of this investigation contributed to a better understanding of the structural critical conditions related to this new deck typology.

Keywords: Composite bridge; Space truss; Circular hollow section; Bending moment; Curvature.

1. Introduction

Aesthetics and environmental integration are nowadays key parameters for most of the bridge designers. The demands related to visual and noise impact and considerations for traffic maintenance during construction are aspects that may be explored when choosing between a concrete and a composite solution, both acceptable in structural and functional terms. However, the possible advantages of composite bridges must be explored together with the deck typology and the erection scheme, in order to face the competitiveness of concrete solutions [1].

In recent times, the use of composite trusses, mainly adopting tubular members has been increasing in bridge design due to:

1. Aesthetical qualities related to lightness and transparency;
2. Adaptability to functionality conditions, namely in double decks for highway and railway traffic [2];
3. Developments in cutting and welding technologies;
4. Increases of the use of high strength steels and lightweight concrete [3].

The aim of this paper is to contribute for the study of composite truss bridge decks, mainly regarding its structural behavior. A loading test performed at a scale model of a composite truss bridge deck will be described. Some brief design cases using this deck typology will also be presented.

2. Composite Truss Decks

Some examples of composite bridge decks, in which the main supporting structure is made from a steel truss, are presented in this section.

The innovative design of the Lully viaduct results in a light and transparent structure made of a triangular cross-section fabricated entirely from unstiffened circular hollow sections. Each twin space truss as a typical span of 42.75m and a slenderness L/H of approximately 13. The cross-section is 2.9 m high and 12.0 m wide and is supported by a single slender pier. The largest diameters and thickness of the tubes are 500 mm and nearly 70 mm respectively. One of the major difficulties was related to the design of the complex KK joint connections between the chords and diagonals, mostly regarding fatigue verifications. Therefore, geometry calculations, computed guided cutting and edge preparation of the tubes were necessary in order to perform fully penetration welds [4].

The steel truss was assembled from ground level by crane trucks with a building speed of one full span every two weeks. Concrete pumping moved at the same speed as the truss erection with use of mobile formwork. Every stage corresponded to half a span and took one week long.

* e-mail: joaopedrobraz@gmail.com

Fig. 1 - The Lully Viaduct, Switzerland.

Some bridge designers have chosen to use cast steel joints for connecting tubular elements. Although less efficient from an economic point of view, the casting process allows an optimal design of the joint according to the flow of internal forces, which can lead to an alternative solution [5].

Cast steel joints were applied at the Nesenbachtal Bridge, shown on Fig. 2. With a total length of 151 m and a main span of 49.5 m, the bridge structure is made entirely from tubular elements made, including the piles. The tubes diameter varies between 193.7 mm and 323.9 mm. The diagonals connect directly to the concrete slab by "saw-tooth" connections, due to the absence of upper chords.

Fig. 2 - The Nesenbachtal Bridge, Germany.

The bridge over the Roize region is considered by many bridge designs as a benchmarking reference due to its innovating structural concept. The composite truss bridge deck, of the authorship of Jean Muller, follows a remarkable modular concept. Each steel module is formed by four tubular diagonals made of steel plates connected by t-butt welds, a 4 m length bottom chord segment with irregular hexagonal shape and an I-shaped plate girder with welded shear studs to provide composite action. The bridge forms a continuous beam system with a span distribution of 36 m, 40 m and 36 m. The bridge deck cross-section is 2,38 m high and 12,20 m wide. In order to considerably reduce the steel elements thickness, external longitudinal prestress tendons were adopted. The concrete deck was also constructed using prefabricated slabs of high performance concrete, which helped to reduce the selfweight of the superstructure [6].

Fig. 3 - The Roise Bridge, France.

3. Experimental Investigation

For the present thesis, a test specimen consisting of a scale model of a composite truss bridge deck was set up and tested to collapse. This section of the paper provides a summary of the experimental procedures that were accomplished at the university's laboratory.

3.1. Description of the Test Specimen

As shown in Fig. 4, the test specimen was a global isostatic beam system, with a middle span of 6 m and a cantilever span of 1,5 m. The specimen was a space truss formed by steel circular hollow sections (CHS) connected to a concrete slab with width and thickness of 1100 mm and 70 mm respectively. The longitudinal reinforcement in each face of the slab consisted of #5 bars spaced of 100 mm. Two rows of shear studs spaced at approximately 180 mm were welded to both top chords, in order to provide composite behavior. All the connections between the continuous chords and the diagonal members were welded connections made on site, avoiding the use of stiffener elements. The top chords were also connected to lateral brace members. The dimensions of the main steel elements are shown in Fig. 4. The geometry of the inferior KK joints between the diagonals and the bottom chord is also presented.

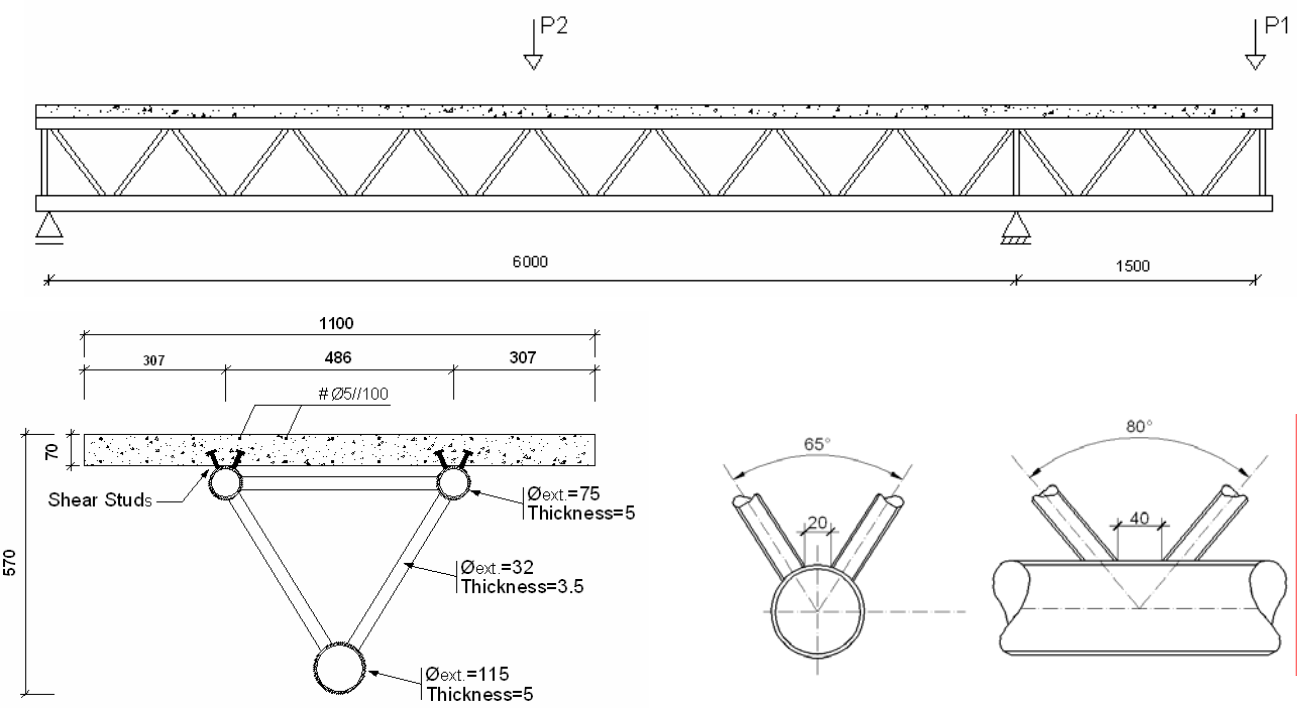

Fig. 4 - Specimen longitudinal shceme, cross-section and inferior KK joint geometry (mm).

3.2. Fabrication of the Test Specimen

The described steel truss had been previously assembled in the extent of another academic investigation. Therefore, only the construction of the concrete slab is covered in the present work.

The construction of the composite truss proceeded as follows:

1. The steel structure was lifted and positioned over the concrete supports.
2. The wood formwork was set up and the steel reinforcement assembled.
3. The slab was concreted in-situ with no use of temporary shores.
4. The concrete slab was manually leveled.

3.3. Material Properties

Material testing was performed to determine the actual material properties.

Tension tests were performed on the steel tubes and #5 reinforcement bars. Fig. 5 shows the results of these tests.

Concrete for the slab was provided by a local ready-mix supplier. The 28-day compressive strength of the concrete was 38.4 N/mm^2 while, at the time of the load tests, the compressive strength was 48.1 N/mm^2, as determined by material testing.

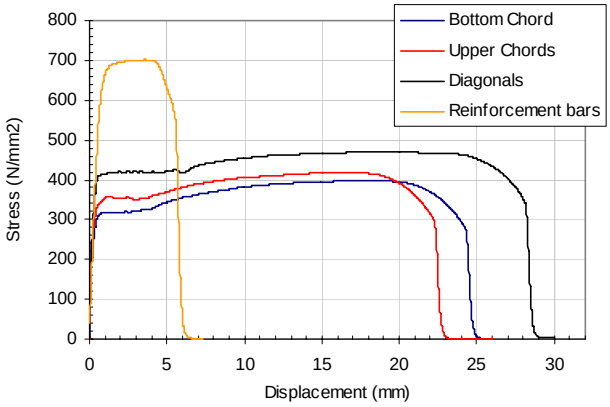

Fig. 5 - Stress-displacement relationship from material testing.

3.4. Instrumentation Plan

During the load tests, strains and deflections were measured at various locations along the structure. Strains were measured using resistive foil strain gauges while vertical displacements were monitored by linear displacement potentiometers located under the load application points. All the instruments were attached to a data-acquisition system controlled by a personal computer. Fig. 6 shows the locations were strains were measured at the intermediate support section.

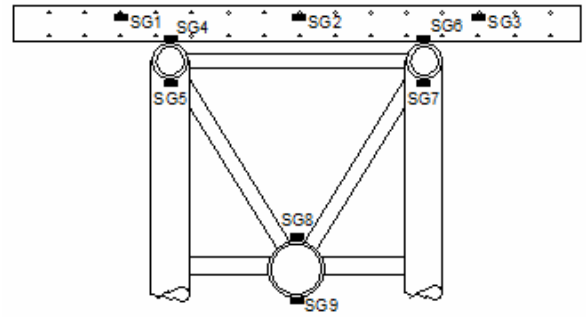

Fig. 6 - Location of strain gauges at support section.

Figure 7 shows the test specimen and loading scheme prior to testing. Roller-type supports made of steel bars were used to allow free rotation and translation in the horizontal direction. Two hydraulic jacks were assembled for loading of the test specimen. Each jack was connected to an individual pumping station, which allowed the application of two independent loads. The correct distribution of loading was achieved using a spreader steel beam placed on the top of the slab. Load incrementation was applied manually at both stations.

The specimen was loaded incrementally at both loading points until a loading value corresponding to the ultimate moment resistance of the support section was achieved. After that, loading at the cantilever end was fixed and incrementing of middle span loading was resumed. Loading at middle span was interrupted when the collapse of the structure is observed.

Figure 8 illustrates the corresponding shear force and bending moment diagrams, due to the planned loading fixture.

Fig. 7 - Test set-up and loading fixture.

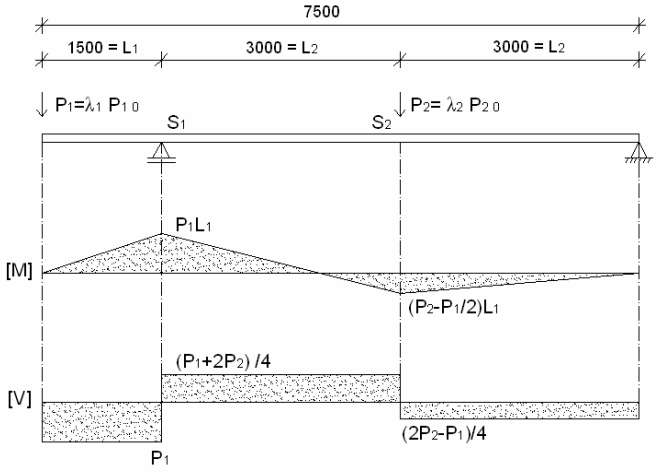

Fig. 8 - Loading scheme and corresponding stresses.

4. Numerical Analysis

Prior to the loading of the test specimen, a numerical analysis was performed to estimate the flexural capacity of cross sections, as well as to predict the vertical displacements of the structural system.

4.1. Moment Curvature Analysis

The purpose of the moment-curvature analysis was to calculate the ultimate moment resistance of the cross sections and to obtain an approximation for some expected behaviors, such as cracking of the concrete slabs and plastification of the steel chords. For purpose of calculation, simplifications were made in the geometry of the CHS members. Slippage between the steel tubes and the concrete slab was not considered.

A numeric program was developed to perform moment curvature analysis for the composite section. The following provides a brief description of the program steps and main assumptions:

1. The cross section is divided into a number of layers, each one corresponding to a particular material, as shown in Fig. 9.
2. An applied moment is selected.
3. A curvature is selected, for which the resistance moment will be calculated.
4. A depth to the neutral axis is selected.
5. The strain at each layer is calculated, assuming a linear strain distribution.
6. The stress at each layer is calculated, on the basis of the appropriate constitutive relationship for each material.
7. The stresses are integrated to obtain the net force of the section.

8. The resistance moment is calculated from the stresses
9. The equilibrium equations for pure bending are resolved: $N_{Ed}=N_{Rd}=0$; $M_{Ed}-M_{Rd}=0$.
10. If equilibrium is not satisfied, steps 3 through 9 are iterated.

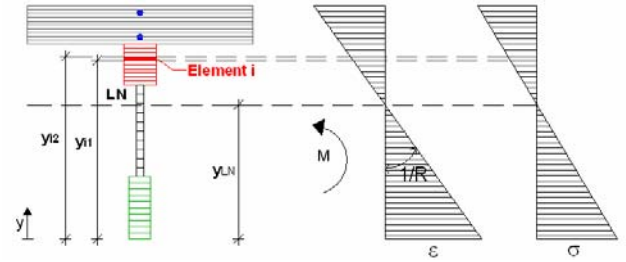

Fig. 9 - Discretization of cross section for numerical analysis.

The material models for the steel tubes and the reinforcing bars were input as bi-linear stress-strain relationships as defined in EC3 [7].

As for the concrete, different mechanical behaviors were considered, according to the nature of the stresses. Therefore, strain-hardening and strain-softening relationships were established when subject to compressive stresses [8]. The "Tension-stiffening effect" was not considered for purposes of simplification.

Figures 10 and 11 show the moment-curvature diagrams obtained from the iterative method previously described.

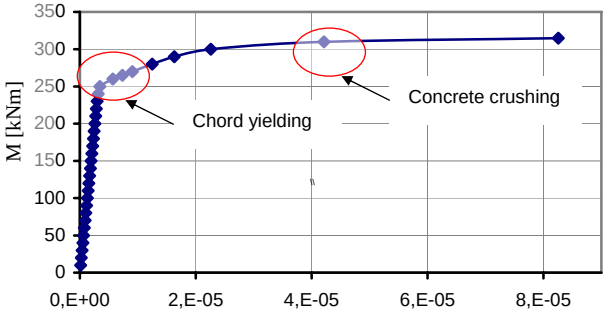

Fig. 10 - Moment-curvature diagram for positive bending moments.

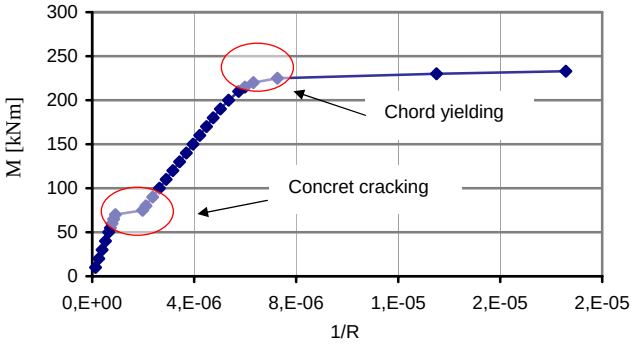

Fig. 11 - Moment-curvature diagram for negative bending moments.

4.2. Structure Displacements

The structure vertical displacements were predicted using the known theorem of virtual works:

$$\delta = \int \frac{1}{R}\overline{M} + \frac{V}{A'G}\overline{V}dx \qquad (1)$$

where the shear area is calculated according to the "equivalent web area" for a Warren-type truss beam. For eq. (1), inelastic bending strains (curvatures 1/R) are included, while shear strains were considered as elastic only.

5. Experimental Results

The following section provides general observations made through the experimental tests and the numerical results obtained.

5.1. Load-Deflection Data

Figures 12 and 13 show the load-deflection curves obtained from the loading test.

As may be seen in Fig. 12, the load-displacement response of the end section is nearly linear until a deflection of 14 mm was reached, which corresponded to an applied load of approximately 120 kN. This results match with the numerical analysis, since the predicted load value for the yielding of the bottom chord was 127 kN. Further indication of the yielding of the bottom chord is given by the strain data analysis. After this level, the system stiffness decreased significantly until the ultimate load of 167 kN is reached with a maximum observed deflection of 44 mm at the end section.

The graph in Fig. 13 shows a linear response for the midspan section during the increment of both loads. After reaching the maximum load applied at the cantilever, the increase of deflections is observed due to the transfer of stress to the positive moment region. However, the structural system reached collapse before the midspan section could reach a level close to his maximum bending capacity. Therefore, the ultimate load for positive moment region could not be obtained. It was observed a maximum deflection of 33 mm at midspan section.

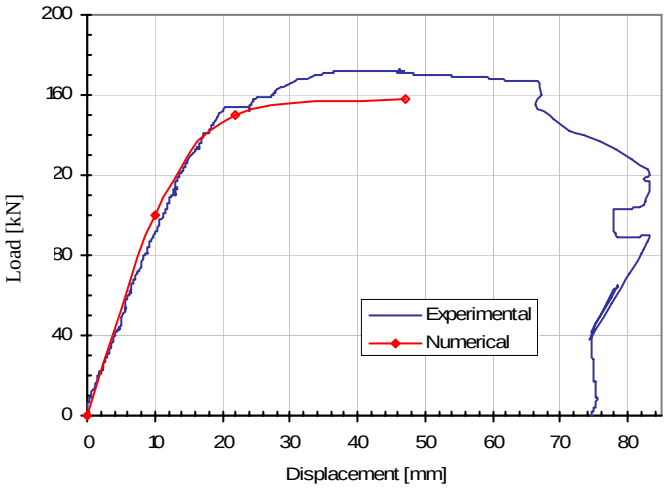

Fig.12 - Load-displacement results for the end section.

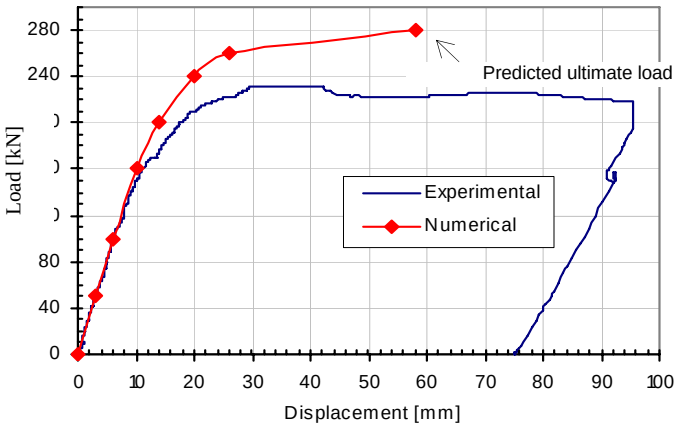

Fig. 13 - Load-displacement results for middle span section.

5.2. Failure Modes

The cracking of the concrete slab occurred for an applied load of 42 kN, close to the theoretical cracking load of 50 kN obtained from the numerical analysis.

The system collapse occurred for cantilever and midspan loads of 167 kN and 235 kN respectively, for which the support section reached his ultimate flexure capacity with rupture of the longitudinal reinforcement.

The support section couldn't achieve the required ductility behavior since the local failure modes observed at the steel truss prevented the stress redistribution to the midspan zone. The system was therefore unloaded at this point, due to the drop in applied loads.

The local failure mode corresponded to the shear failure of the bottom chord at the KK-shaped joint closest to the intermediate support, together with the buckling of the compressed diagonals, as shown in Figures 14 and 15.

It is important to notice that failure of the weld roots was not observed in any location of the structure.

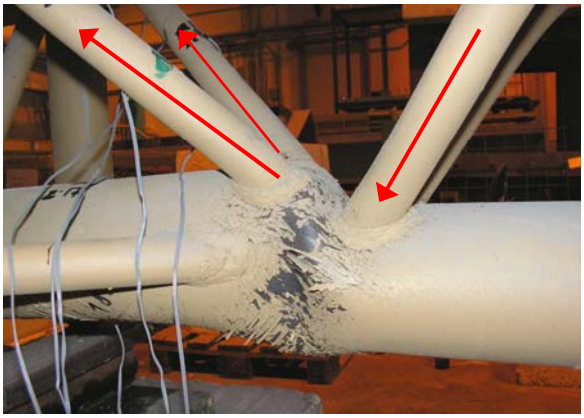

Fig. 14 - Chord shear failure next to intermediate support.

Fig. 15 -Buckling of compressed diagonals.

5.3. Strain Data

Figures 16 to 19 show the strain results monitored at different locations of the test specimen.

Figure 16, corresponding to the strains installed at the bottom and top of the lower chord located at the midspan, shows that the strain profile is highly linear in this region. This indicates that it would have been possible to engage significant deflection at the midspan section after the yielding of the lower chord, due to the considerable displacements obtained from elastic behavior.

As seen in Fig. 17, concrete cracking in negative moments region occurred for an applied load of 42 kN, which corresponds considerably to the estimated values since the cracking load, was calculated as 50 kN. The same graph shows the lack of ductility of the reinforcement bars due to the sudden interruption of the load-strain curve for the ultimate load of P_2=235 kN.

As seen in Fig. 18, the bottom chord in negative region has shown a linear behavior until an applied load of approximately 95 kN was achieved, resulting in an increase of the slope of the load-strain curve. Although showing a ductility behavior after the yielding of the most distanced fiber, the section reached complete plastification before the maximum applied load was reached. Analytic results show that, for a load case of P_1=167 kN; P2=235kN, the bottom chord reaches a corresponding compressive force of 453 kN, very close to the $N_{PL,Rd}$ value.

Figure 19 shows the strain data measured at four diagonals of the space truss, each reading corresponding to one element. Results indicate a linear load-strain relation for the compressed diagonals for applied loads within P_2=167 kN (maximum load applied at the cantilever). Readings show a first change in the graph's slope due to the interruption of loading at the cantilever. A second slope change for P_2=210 kN suggests that these elements began to respond in post-critical behavior from this point forward. Analytical results show a maximum compressive strength of 85 kN at the diagonals for an applied load of 167 kN, very close to the design buckling resistance, matching with the test results.

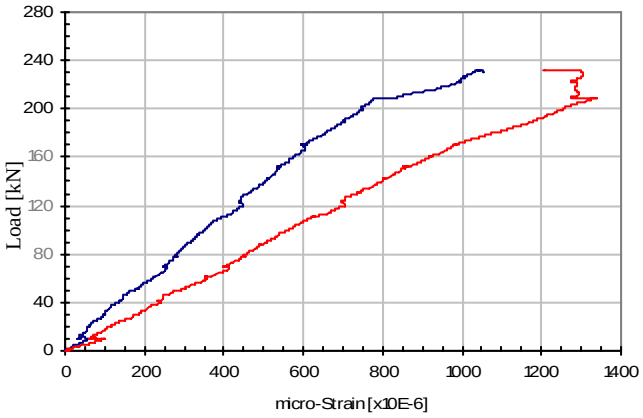

Fig. 16 - Strain data in the reinforcement bars at the support region.

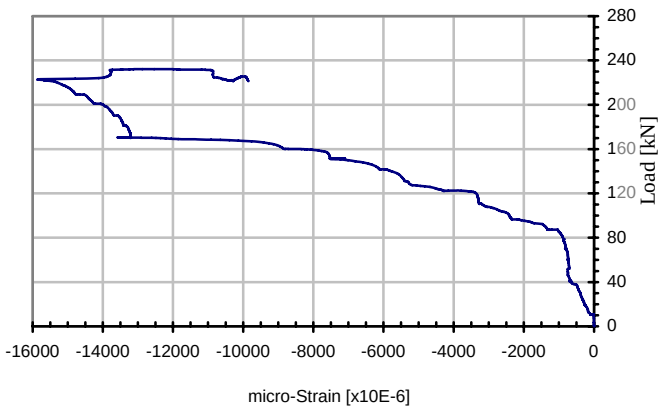

Fig. 17 - Strain data in the bottom chord at the support region.

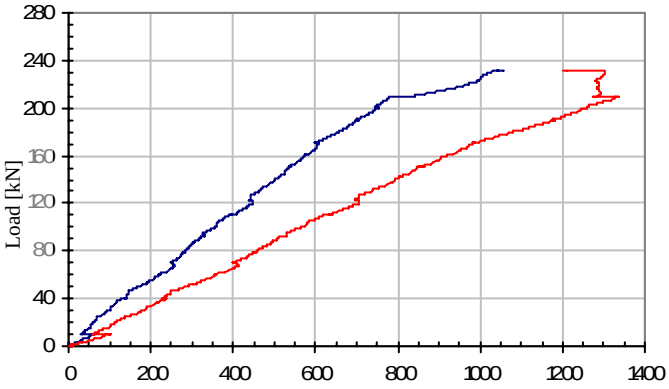

Fig. 18 - Strain data in the bottom chord at the midspan region.

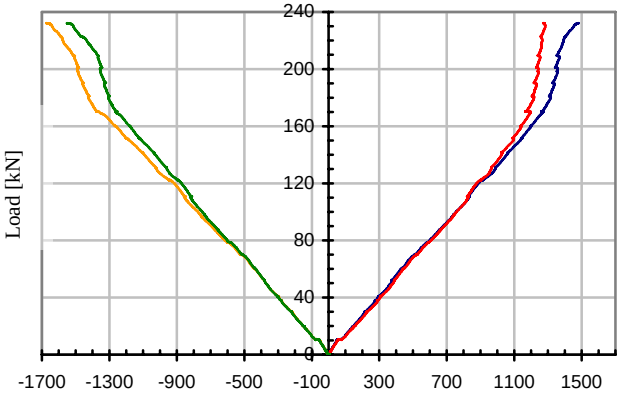

Fig. 19 -Strain data at the diagonals.

6. Conclusions

Composite truss bridges stand out mainly for their aesthetic qualities and innovating design, which make them competitive when facing traditional solutions.

The present work tries to give a contribution to the study of composite truss decks regarding the structural response to the ultimate limit states.

Moment curvature analysis showed a good prediction for $M_{cracking}$ and for the ultimate flexural capacity at the support region as for the vertical structural displacements, mainly during elastic regime.

All the welds between tubular elements showed good resistance during the load test. No failures at the weld roots were observed.

Longitudinal reinforcement was clearly insufficient to allow a full redistribution of bending moments, since unpredicted local failure modes occurred during the load test, preventing the midspan region from

reaching higher solicitations. Furthermore, test results showed that tubular diagonals responded at post-critical regime, which was later confirmed by strain data analysis.

To achieve a good ductility performance, verifications must be made regarding not only to the global structural behavior but also possible local failure mechanisms located at the truss joints.

Appendix A - Analytical Model of the Structure

With purpose of comparing with the test results, elastic analyses were carried out with a 3D model of the structure, as presented in Fig. 20.

The steel truss was modeled with frame elements with no torsional resistance and the concreted slab with four-node shell elements. The frame and shell elements were connected by rigid links because the model was assumed to behave as full interaction. The steel truss frame elements were connected by stiffened joints in order to account for the secondary stresses at the tubes, due to local bending. Cracked analysis was made by simply discarding the corresponding shell elements. However, more accurate calculations can be made by means of non-linear push-over static analysis, available in the software.

Calculations were carried out by the structural analysis software *SAP2000*, developed at Harvard University.

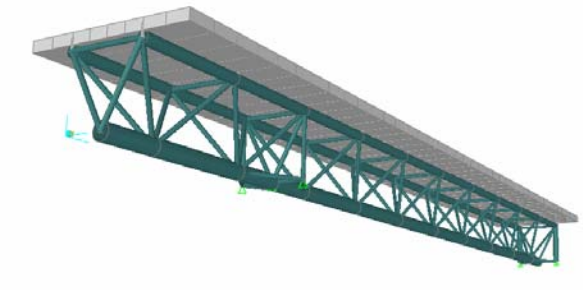

Fig. 20 - Analytical model of the test specimen.

References

[1] Reis, A.J. – "Bridge decks: composite systems for improved aesthetics and environmental impact", Composite Bridges: State of the Art in Technology and Analysis, Proceedings of the 3rd International Meeting, Colegio de Ingenieros de Caminos, Canales y Puertos, Madrid, 2001.

[2] Reis, A.J. - "Steel concrete composite bridges: options and design issues", 7th International Conference on Steel Bridges, Guimarães, Portugal, 2008.

[3] Cruz, Paulo; Reis, A. J. – "Pontes com tabuleiros misto aço-betão: utilização de betões leves de alto desempenho", 3º Encontro de Construção Metálica e Mista, Aveiro, 2001.

[4] Dauner, Hans G.; Decorges, G.; Oribasi, A.; Wéry, D. - "The Lully Viaduct, a Composite Bridge with Steel Tube Truss", Journal of Constructional Steel Research, Paper 55, 1998.

[5] Kuhlmann, Ulrike; Günter, Hans-Peter - "Welded circular hollow section (CHS) joints in bridges", Proceedings of the 10th International Symposium of Tubular Structures, Madrid, 2003.

[6] Montens, Serge; Causse, Gilles; Bouchon, Pascal - "Le pont experimental sur la Roize", Bulletin Ponts Métalliques, Nº 15, France, 1992.

[7] *Eurocode 3 - Design of steel structures - Part 1-1:General rules and rules for buildings"*, EN 1993-1-1, European Committee for Standardization, Brussels, 2005.

[8] Pedro, José Oliveira – "Pontes atirantadas mistas: estudo do comportamento estrutural", Tese de Doutoramento em Engenharia Civil, IST, Lisboa, 2007.